

# Monte Carlo simulation study of diblock copolymer self assembly

George J. Papakonstantopoulos<sup>1\*</sup>, Kostas Ch.

Daoulas<sup>2</sup>, Marcus Müller<sup>2</sup>, and Juan J. de Pablo<sup>3</sup>

<sup>1</sup>*Department of Chemical Engineering,*

*University of Wisconsin-Madison, Madison,*

*WI 53706 - Currently: Department of Materials Science  
at Goodyear Tire & Rubber Company, Akron, OH, 44305*

<sup>2</sup>*Institut für Theoretische Physik, Georg-August Universität,*

*37077 Göttingen, Germany and Department of Physics,*

*University of Wisconsin-Madison, Madison, Wisconsin 53706,*

*USA - Currently: Department of Polymer Theory,*

*Max Planck Institute for Polymer Research, Mainz, P.O. Box 3148*

<sup>3</sup>*Institut für Theoretische Physik, Georg-August Universität,*

*37077 Göttingen, Germany and Department of Physics,*

*University of Wisconsin-Madison, Madison, Wisconsin 53706, USA and*

<sup>4</sup>*Department of Chemical Engineering,*

*University of Wisconsin-Madison, Madison,*

*WI 53706 - Currently: Institute of Molecular Engineering,*

*University of Chicago, Chicago, IL, 60637*

(Dated: May 11, 2019)

---

\* Author to whom correspondence should be addressed. Electronic mail: [gjpapakonsta@gmail.com](mailto:gjpapakonsta@gmail.com)

## Abstract

A technique is presented which maps the parameters of a bead spring model, using the Flory Huggins theory, to a specific experimental system. By keeping only necessary details, for the description of these systems, the mapping procedure turns into an estimation of a few characteristic parameters. An asset of this technique is that it is simple to apply and captures the behavior of block copolymer phase separation. In our study this mapping technique is utilized in conjunction with a Monte Carlo (MC) algorithm to perform simulations on block copolymer systems. The microphase separation is investigated in the bulk and under confinement, on unpatterned and patterned surfaces.

PACS numbers:

Keywords: block copolymers, nanolithography, three dimensional nanostructures, mapping technique, coarse graining, self assembly

## I. INTRODUCTION

The combination of two or more different types of polymers as blends or copolymers to obtain materials with improved properties is a common procedure. In most cases, however, blending two different kinds of polymers can result in phase separation. In the case of diblock copolymers (molecules that consist of two distinct polymer chains covalently bonded at one end), because of connectivity constraints, the self-assembly results into domains that exhibit ordered morphologies of a variety of ordered structures. Depending on their chain asymmetry and the Flory-Huggins parameter, which is a measure of the incompatibility of the different type of monomers [1], these structures can be lamellae, cylinders, spheres, gyroids. When the self-assembly is performed on patterned surfaces, the pattern can be used to guide the block copolymer morphology giving precise control of the process resulting in perfect, defect free structures that are similar to the bulk morphology or completely new structures. These morphologies are especially suited for a number of applications in nanofabrication such as nanowires [2], photonic crystals [3], quantum dots [4], magnetic storage [5].

Several theories have been proposed to study these materials. The classical theoretical method to treat these systems is based on the Flory and Huggins lattice mean-field model [1]. This theory has been the basis of considerable efforts to develop methods able to describe the phase separation of polymer blends. One such popular method is the self consistent field (SCF) technique [6]. However, the SCF theory is built on a number of assumptions. For example, the SCF theory employs a Gaussian model for polymer chains to describe the entropy of the system, and it adopts a Flory-Huggins interaction parameter to account for energetic contributions to the free energy of the system. This theory does not take into account fluctuation effects. Recently though, a new particle based SCF method has been developed [7, 8, 9] which retains the advantages of the SCF but it also includes fluctuation effects and maintains explicitly information about the molecular conformations.

Molecular simulations such as Monte Carlo (MC) and molecular dynamics (MD) have been utilized in the past for the investigation of block copolymer self assembly. Computer simulations play a significant role in testing theoretical models and in interpreting experimental results. A study of these systems on a molecular level is necessary and simulations are an indispensable tool to visualize the molecular mechanism of the self-assembly of the block copolymers. They are able to explain and predict the three dimensional final geome-

try and give details on chain conformational properties. These techniques highlight the role of fluctuations and provide insights into the local structure. Another important feature of molecular simulations is that structural and thermodynamic quantities are simultaneously accessible and parameters can be varied independently. They also provide the exact solution of a model which can be fully atomistic or coarse grained. A fully atomistic description of block copolymer chains is yet computationally prohibitive, if we desire to study chains of sufficiently large molecular weight on length scales which usually range from the nanometer to micrometer regime and enormous time scales required for equilibration. But one more important issue is the fact that the results are quite sensitive to the intermolecular potentials which is a serious limitation [10].

A coarse grained approach is ideal due to the fact that only important details are kept and others, such as chemical details, are neglected. Of course the issues that exist with the choice of the potential for the atomistic description are transferred to the coarse grained model if results obtained from atomistic simulations are used for the mapping procedure. To circumvent this problem we can use as an input thermodynamic or structural data from available experimental results of the system that we choose to study rather than atomistic simulations. An important issue that has to be noted though is the fact that results from the coarse grained model can be predictive only to the extent of the model parametrization.

A common technique employed when using coarse grained models is the lattice Monte Carlo [11, 12, 13, 14, 15, 16]. This algorithm has the advantage to be computationally convenient and fast and give the ability to simulate large systems. However, these models can introduce artificial spatial anisotropies. An additional compromise is that the systems must be studied in an isochoric ensemble while some problems are more easily investigated in an isobaric ensemble.

An extension of the simple lattice Monte Carlo simulations is the bond fluctuation model. The chains are more “flexible” since the monomers are not restricted only to the closest lattice sites. This technique has been vastly used and significant calculations on phase separation of blends and block copolymers both in the bulk and under confinement have been performed [17, 18, 19].

Apart from Monte Carlo, molecular dynamics have also been utilized to study block copolymer self-assembly. One method used to investigate the phase behavior of diblock copolymers is the discontinuous molecular dynamics [20, 21, 22]. This technique converges

quite fast but at the same time is limited to small chain lengths due to equilibration efficiency. One more strength of the discontinuous molecular dynamics is its capability to predict the dynamical pathway along which a block copolymer melt finds its equilibrium structure after a temperature quench. Going further in simulation complexity, Grest et al. [23, 24] have performed molecular dynamics simulations aided by Monte Carlo identity exchange move focusing on the study of block copolymer chains in the disordered and lamellae phase in the bulk.

In this manuscript we present a facile and incomplex procedure to map the parameters of a coarse grained model to theory and connect our results to specific experimental systems. After obtaining the values of the necessary parameters we utilize a Monte Carlo algorithm in continuum with specific moves that are proven to be efficient for the study of these systems [25, 26]. We turn to continuum simulations to avoid problems that cannot be dealt with lattice Monte Carlo. A few of the advantages of resorting to continuum description are the ability to use an isobaric ensemble, the investigation of systems such as branched or crosslinked polymers since an off lattice simulation would be more realistic and also the study of the effect of volume differences between species. In a continuum description we have better means to investigate local properties and interphase local structure. Upon describing the suggested mapping methodology, our bead spring model will be used to reproduce experimentally retrieved results such as lamellae and cylinder formation on unpatterned and patterned surfaces.

## II. SIMULATION DETAILS

The segments of the polymer molecules interact pairwise via the 12-6 Lennard-Jones truncated potential energy function, shifted at the cutoff  $r_c = 2^{1/6}\sigma$ . This renders the segments repulsive to one another and the cutoff is small so that the number of interacting neighbors is quite small.

$$U_{nb}(r) = \begin{cases} 4\epsilon \left[ \left(\frac{\sigma}{r}\right)^{12} - \left(\frac{\sigma}{r}\right)^6 \right] - U_{LJ}(r_c), & r \leq r_c \\ 0, & r > r_c \end{cases} \quad (1)$$

where  $\varepsilon$  and  $\sigma$  are the Lennard-Jones parameters for the energy and the length respectively and  $r$  the distance between the segments. The parameter  $\sigma$  has a value of  $\sigma = 1$  while  $\varepsilon$  is an adjustable parameter. The bonding energy between consecutive segments in the same chain is given by

$$U_b(r) = \frac{1}{2}k(r - \sigma)^2 \quad (2)$$

with bond constant  $k = 2 \cdot 10^3 \varepsilon / \sigma^2$ .

The surface potential is described by

$$U_{surf}(r) = \pm \frac{\Lambda f(x, y)}{\varepsilon R_e} \exp\left(\frac{-z^2}{2(\varepsilon R_e)^2}\right) \quad (3)$$

where plus and minus signs correspond to PS and PMMA substrate interactions. The coefficient  $\Lambda$  characterizes the strength of the interaction while the function  $f(x, y)$  provides the pattern of the substrate.

The systems studied consist of chains of  $N = 32$  beads and the density was chosen to be  $\rho = 0.7$  for convenience of computation. The temperature was selected to be  $T = 2.0$ . For brevity all quantities in the manuscript are reported in LJ reduced units.

Specific Monte Carlo (MC) moves have been utilized to overcome severe limitations that traditional MC and molecular dynamics methods are facing in macromolecular systems. Random monomer displacements are used for local movements together with reptation moves in a configuration bias scheme to increase performance. While reptation can be effective in dilute systems of short chains, for intermediate to long chain molecules it is essential to resort to trial moves capable of rearranging inner segments of the polymer. This is particularly important in our present study, where block copolymer chains get trapped after a phase starts to form and sampling the correct structure and arrangement of long chain molecules can be particularly demanding. For this reason double bridging trial moves are implemented [25, 27]. This is a chain-connectivity-altering move which consists of a simultaneous exchange of parts of two neighboring chains. Double bridging allows for effective equilibration of the systems under study and sampling via configurational bias significantly enhances acceptance of the rebridging scheme. The acceptance ratio of the random displacement is kept at 30%. For the double bridging either two or one beads are chosen to be deleted and rebuilt to increase acceptance and depending on the system under study an acceptance ratio of 0.5 to 1.5% is obtained in the case where one bead is chosen.

### III. MAPPING METHODOLOGY

In order to be able to compare results from a molecular simulation of a coarse grained model with theory and experiments it is necessary for a number of parameters of the coarse grained model to be mapped. The first one is the Flory-Huggins parameter,  $\chi N$ , which is a measure of the incompatibility of the segments belonging to different blocks and determines the parametrization of the cohesive interactions. The second is the end-to-end distance of the block copolymer chain and provides the mapping of the length scales. The interaction strength of the surface is regulated by the parameter  $\Lambda N$  and finally the invariant degree of polymerization  $\bar{N}$  controls the strength of fluctuations.

The degree of polymerization is defined as:

$$\bar{N} = \left(\frac{\rho R_e^3}{N}\right)^2 \quad (4)$$

For a usual block copolymer system [8, 28, 29, 30] the value of this parameter is extremely large. Due to computation limitations, we shall not use an exact value of an experimental system for our coarse grained model;  $\bar{N}$  can be increased by either increasing the chain length  $N$  or the density  $\rho$ . We are more interested to show how a realistic system can be mapped and suffice with a lower value for  $\bar{N}$  which will give rise to stronger fluctuations. These fluctuations, even if they affect the occurring morphologies they still allow for a clear pattern formation which as will be shown later is quantitatively in agreement to experimental results.

The next step is to obtain the length scale for our model, which, as was mentioned, is  $R_e$ . The value of  $R_e$  can be easily determined from a simulation of the blockcopolymer after the Lennard-Jones parameters have been mapped to correspond to specific  $\chi N$ . For example, for a density of  $\rho = 0.7$ , chain length  $N = 32$ , and chain asymmetry of  $f = 15/32$ , the system of  $\varepsilon_{AA} = \varepsilon_{BB} = 0.022$  and  $\varepsilon_{AB} = 1.0$  it is found that  $R_e = 7.8$ , while for  $\varepsilon_{AB} = 10.0$  we obtain  $R_e = 8.1$ .

The strength of the surface interaction  $\Lambda N$  for our simulations is obtained by considering a PMMA-PS block copolymer of chain length  $N = 32$  and  $\chi N = 36.7$  confined between two uniform substrates, one PMMA-attractive and the other PS-attractive substrate, which form a sandwich geometry. We calculate the density profile of the polymer segments perpendicular to the substrates. The surface energy is determined via the convolution of the polymer-

substrate interactions and the estimated density profile.

$$\Delta E = \int dz U_{surf}(\rho_A - \rho_B) \quad (5)$$

To obtain an order of magnitude estimate for the surface free energy differences, we utilize the adsorption energy per unit surface of a PMMA melt on a silicon oxide substrate, which as found in the literature [31], is  $0.018k_B T/nm^2$ . In order to match this value we choose  $\Lambda N = 3.0$ , which for the system  $\varepsilon_{AA} = \varepsilon_{BB} = 0.022$  and  $\varepsilon_{AB} = 1.0$ , corresponds to  $\sim 0.016k_B T/nm^2$ . In Figure 1 the density profile and the convolution of the surface energy with the difference of density profiles is given.

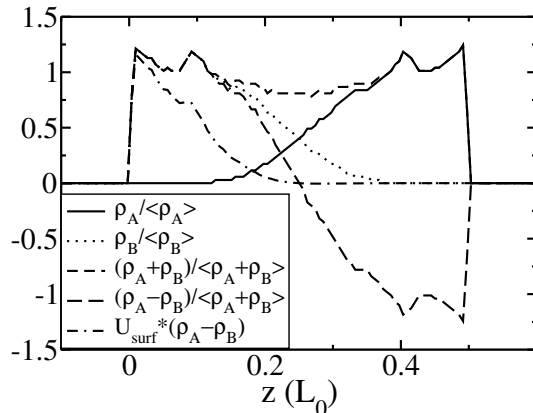


FIG. 1: Distribution of density for the block copolymer system in the “sandwich” system defined in the text. The convolution of the density profile with the polymer-surface interaction used to obtain the free energy differences and map  $\Lambda N$  is also plotted.

To map the Flory-Huggins parameter,  $\chi N$ , we perform semigrand canonical ensemble simulations on a blend of unlike A and B homopolymers, and change the energy interaction parameter  $\varepsilon_{AB}$  of the Lennard Jones potential between the beads of polymer chains. The chain length is chosen sufficiently smaller in this set of simulations for efficiency. The volume fraction of the unlike beads, from the first derivative of the Flory-Huggins free energy, will follow:

$$\chi N = \frac{\ln(\phi/(1-\phi))}{2 \cdot \phi - 1} \quad (6)$$

which at the strong segregation regime reduces to:

$$\phi \sim \exp(-\chi N) \quad (7)$$

Initially chains of the same type are inserted with the aid of configuration bias in the simulation box. When the desired density is reached, 50% of the chains are selected to be of one type and the rest of the other. The opposing type interactions are “switched on” in this way. Next the system is simulated under the semigrand canonical ensemble. By virtue of the structural symmetry of the blend components, the semigrand ensemble reduces to an identity exchange type of move and the acceptance criterion involves only the difference in initial and final energy. By knowing the desired value of  $\chi N$  the energy interaction parameter  $\varepsilon$  can be modified until the volume fraction occurring from the simulation fulfills the previous relation.

In the following, we will exhibit how the values of the energy interaction parameter  $\varepsilon$  of the Lennard Jones potential can be estimated so that our bead spring model represents a system of a desired Flory-Huggins parameter. The experimental system that will be compared is composed of PS-b-PMMA chains of such molecular weight giving a  $(\chi N)_{exp} = 36.7$  [8, 28, 29, 30]. The chain length chosen for the block copolymer self assembly simulations is  $N = 32$ . The described mapping methodology is performed using smaller polymer chains of length 4 and changing  $\varepsilon$  until the volume fraction is

$$\phi \sim \exp(-(\chi N)_{experimental} * 4/32) \quad (8)$$

From our calculations we find that the values of the Lennard-Jones energy parameters that correspond to this  $(\chi N)_{exp}$  are  $\varepsilon_{AA} = \varepsilon_{BB} = 0.022$  and  $\varepsilon_{AB} = 1.0$  using the test case  $N = 4$ . We continue by performing semigrand canonical simulations using the extracted parameters, but for different chain lengths in order to recover the value of  $\chi$  as a function of  $N$ . From Figure 2a we see that the value of  $\chi$  depends on molecular weight. This molecular weight dependence can be described by [32, 33, 34]:

$$\chi = \chi_{\infty} + k * N^{-1/2} \quad (9)$$

From this result it is clear that for the calculations of the mapping procedure we have to use polymer chains of the same length as the ones that will be used for modeling these systems. However, these simulations are computationally expensive for large chain lengths as was already mentioned. We can perform instead the calculations for a range of smaller chain lengths and then extrapolate to the desired one. The results are plotted in Figure 2. We see that if this molecular weight dependence was not taken into account, then the

mapping procedure would have resulted in a set of parameters giving an incorrect value of  $\chi$ . If we extrapolate the data to  $N = 32$ , we find that  $\varepsilon_{AB} = 284$  for  $(\chi N) = 36.7$ .

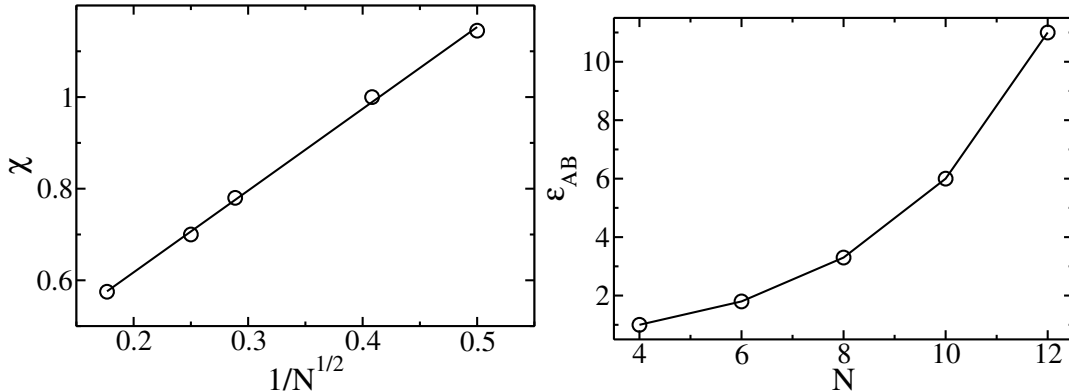


FIG. 2: a)  $\chi$  dependence on molecular weight for a blend of unlike A and B homopolymers system and Lennard-Jones parameter,  $\varepsilon_{AB} = 1$ . b) Value of Lennard-Jones parameter,  $\varepsilon_{AB}$ , in order to obtain  $\chi N = 36.7$  for block copolymer chains of length  $N = 32$  using chain of different lengths for the mapping procedure through semigrand canonical simulation.

We now examine the temperature effect on  $\chi N$ . For a set of temperatures and a series of  $\varepsilon_{AB}$  the value of  $\chi N$  is calculated. Our results are exactly described by a quadratic function in  $1/T$  of the form [35]:

$$\chi(T) = A + B/T + C/T^2 \quad (10)$$

We thus find a non-linearity of  $\chi$  as a function of  $1/T$ . Another interesting point is the fact that for high values of  $\varepsilon_{AB}$  the curves collapse on each other, as can be seen from Figure 3b. This suggests that another way for mapping  $\varepsilon_{AB}$  for a system of  $N = 32$  is to perform the calculations for the mapping procedure at a high  $T$  and then use the collapsed curve to extrapolate the desired value of  $\chi N$  for a specific temperature.

We continue by performing simulations in the semigrand canonical ensemble for a system of chain length  $N = 32$  at temperature  $T = 10$  and for a range of  $\varepsilon_{AB}$ . As can be seen from Figure 4,  $\chi N$  increases as  $\varepsilon_{AB}$  increases. Using the correction from Figure 3b we obtain the corresponding curve for  $T = 2$ . In addition to this mapping technique, we perform an NVT simulation of a symmetric blend of homopolymers and calculate the value of  $\chi N$  from the definition of Flory-Huggins theory for the same range of values of  $\varepsilon_{AB}$ :

$$\chi = \frac{z * \Delta\omega}{kT} \quad (11)$$

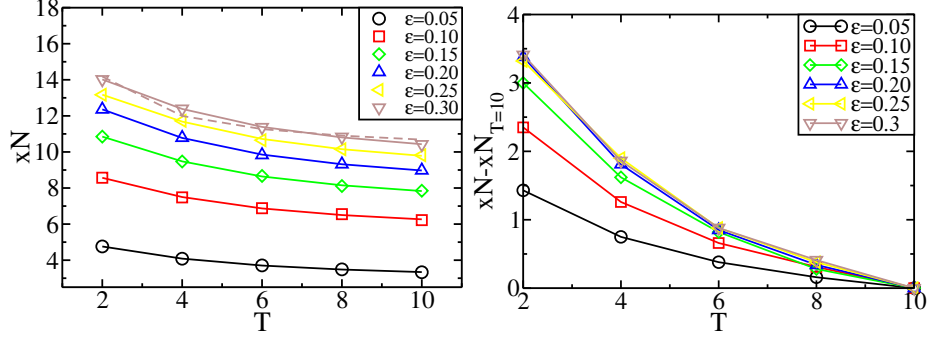


FIG. 3: a)  $\chi N$  with respect to temperature for different values of  $\varepsilon_{AB}$  and for chain length  $N = 32$ . For low values of  $\varepsilon_{AB}$  the curve appears to be linear. The solid lines represent fits with equation 10. The dashed line is plotted for comparison with a linear fit of our data. b)  $\chi N$  with respect to temperature for different values of  $\varepsilon_{AB}$  and for chain length  $N = 32$ . Curves shifted in order for  $\chi N = 0$  zero at  $T = 10$ . Collapse of curves of  $\chi N$  with respect to temperature for high values of  $\varepsilon_{AB}$ .

where  $z$  is the coordination number (the number of nearest neighbors or the average number of sites surrounding an individual segment below the cutoff radius), and  $\Delta\omega = \Delta U_{AB} = \frac{\varepsilon_{AB} - (\varepsilon_{AA} + \varepsilon_{BB})/2}{\varepsilon_{AB}}$  is the energy increment per A-B monomers contact (excess potential energy attributed to the A-B interactions over the number of A-B interactions). From Figure 4 we find that for all the range of  $\varepsilon_{AB}$  values, the difference of the two methodologies is small. In order to verify the agreement of these two methods we perform a calculation with the last mapping methodology using  $\varepsilon_{AB} = 284$  and we find  $\chi N = 34.8$  in close agreement with our desired result.

We continue our study by investigating how the value of  $\chi$  is affected by the composition and the difference between having a blend or block copolymer. We use the previously described methodology, where  $\chi$  is directly obtained by the definition from the Flory-Huggins theory. First we perform a calculation for a blend system with a composition of 50% and then a symmetric block copolymer system. Two values of  $\varepsilon_{AB} = 1$  and 300 are chosen. We find for both systems that the value of  $\chi$  is the same independent of system type (blend or block copolymer),  $\chi_{\varepsilon_{AB}=1} \cong 0.619$  and  $\chi_{\varepsilon_{AB}=300} \cong 1.096$ . This suggests that the fact that the system is a blend or a block copolymer does not have any effect on the value of  $\chi$ . We perform a calculation for blend systems of compositions 1%, 25%, and 50%. It is found

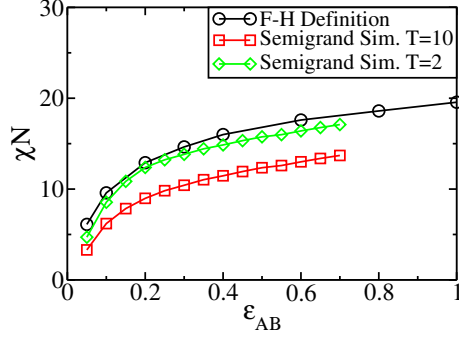


FIG. 4:  $\chi N$  with respect to  $\epsilon_{AB}$  for chains of length  $N = 32$  and for the two methodologies. The technique utilizing the semigrand canonical simulations and the one extracting  $\chi$  as defined from Flory-Huggins theory.

that again the value of  $\chi$  remains constant. This is a special case for our system since the interaction between similar type segments are considered to be identical. In general [36, 37], a composition dependence exists for the Flory-Huggins interaction parameter  $\chi$ .

#### IV. TESTING THE MODEL

As a test system we choose to study the behavior of lamellae forming A-B block copolymer chains on patterned surfaces having the stripe geometry. The mismatch of the pattern spacing  $L_s$  to the block copolymer lamellae period can affect the final structure. In order to proceed with the investigation of this problem, we have to calculate one extra parameter: the block copolymer lamellae period  $L_0$ . Block copolymers chains are inserted between two hard wall surfaces using the configuration bias method. The Lennard-Jones interaction parameters are assigned the values  $\epsilon_{AA} = \epsilon_{BB} = 0.022$  and  $\epsilon_{AB} = 1.0$  and the system is equilibrated (the extraction of these parameters has been shown in the previous Chapter). The block copolymer chain length is  $N = 32$  and comprised of 15 beads of A and 17 beads of B copolymer in order to match chain asymmetry of experimental results [30] for PMMA-PS blockcopolymer. An initial guess for  $L_0$  comes from the literature [30, 38] and is  $1.7 R_e$ .

The  $z$  axis of the simulation box is chosen to be normal to the two surfaces. We perform a  $NPT$  simulation setting the  $x$  direction to be multiple of  $L_{0,guess}$ . The pressure is chosen so that the average density of the system is  $\rho = 0.7$ . Only the  $x$  and  $y$  box lengths are allowed to change keeping the  $z$  length constant. The system is equilibrated and the lamellae period

is found to be  $L_0 = 14.1\sigma$  or  $L_0 = 1.81R_e$ .

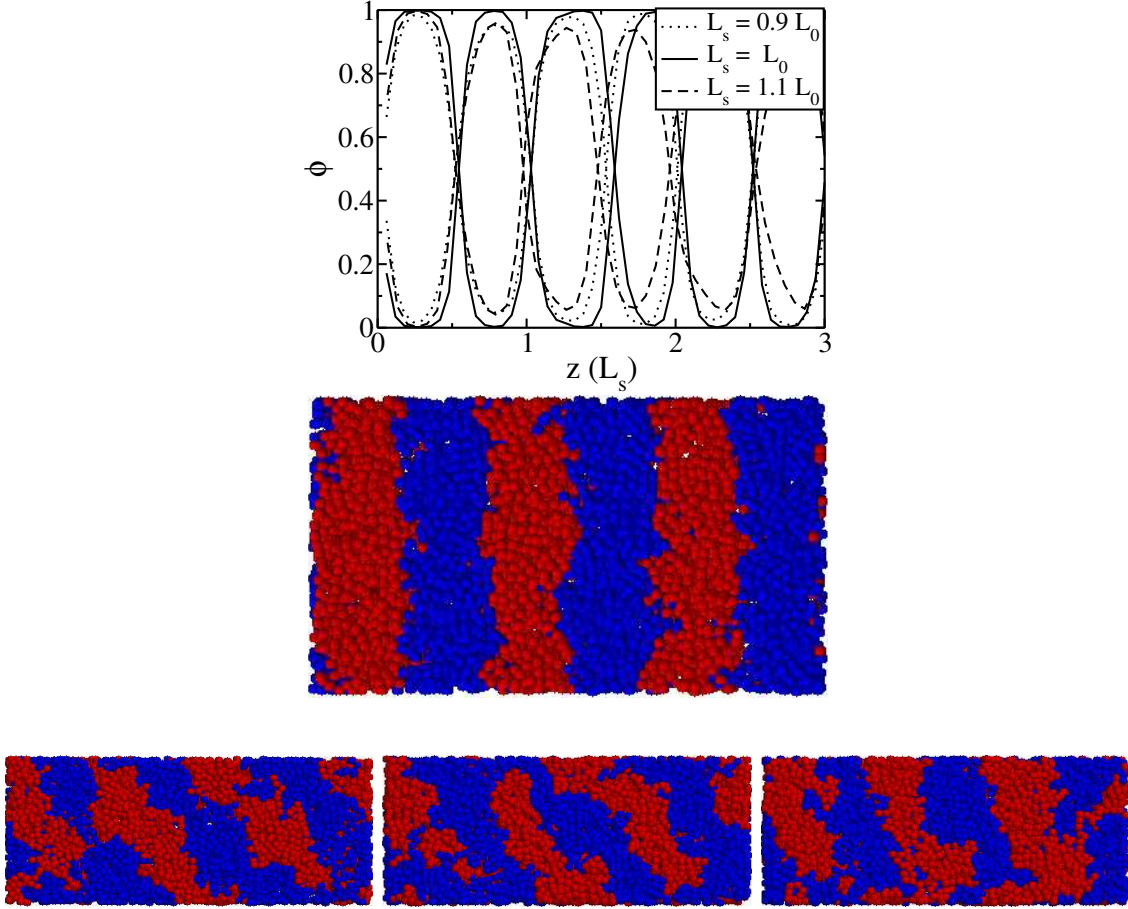


FIG. 5: a) Distribution of volume fraction of a block copolymer on a stripe patterned surface. Results for mismatch of the pattern spacing and the block copolymer lamellae period are plotted for both extensions and compressions. b) Top view snapshot of the block copolymer film simulation on a stripe patterned surface with pattern spacing commensurate to the lamellae period and 10% mismatch. c,d,e) Consecutive sideview snapshots of block copolymer with an increase of pattern spacing of 20%.

We can now proceed with the study of the previously stated problem. The block copolymer is deposited on a patterned surface of stripe geometry with pattern  $L_s$ . A mismatch is chosen between the pattern spacing and the blockcopolymer period ranging from  $-20\%$  to  $+20\%$ . Upon equilibration of the systems the density profile along the normal to the lamellae axis is calculated. The results are plotted in Figure 5a.

Lamellae are obtained for the full spectrum of the previously mentioned “strains”. We find that for both compression and extension, a certain “strain” can be tolerated as seen in Figure

5b. Below or above these critical “strains”, defects arise that are “frozen” as shown in Figures 5c,d,e where subsequent sideview snapshots of the system are plotted. The simulation time between these last configurations is equal to five rouse relaxation times. Similar defects have been observed by experiments under SEM and AFM [30] and quantitative agreement is found with our simulations.

The systems that we investigated so far consisted of block copolymer chains with a chain asymmetry and a  $\chi N$  value that corresponds to the lamellae region of the phase diagram. The natural next step to test our model is to proceed with the investigation of another domain of the phase diagram and more specifically the cylinder regime. We choose values of chain asymmetry and Lennard-Jones interaction parameters that result in the cylinder phase. A chain length of  $N = 32$  is chosen with 22 segments of A type and the rest 10 of B type giving a fraction of 0.3125. The Lennard Jones energy parameters are chosen to be  $\varepsilon_{AA} = \varepsilon_{BB} = 0.022$  and  $\varepsilon_{AB} = 19.0$ , which correspond to a  $\chi N$  of 30.6.

Block copolymer chains are inserted between neutral surfaces. A simulation in the  $NPT$  ensemble was performed changing the axes independently. After equilibration, it is found that  $L_x = \sin(\frac{\pi}{3}) * L_y$ . This relation is necessary in order for the system to be able to accommodate the hexagonal structure of the cylinder phase, which can be seen from geometrical calculations. The cylinder to cylinder spacing was measured to be  $L_{cc} = 2.1R_e$ . The resulting two dimensional density profile is plotted in Figure 6. The hexagonal cylinder morphology is clearly observed.

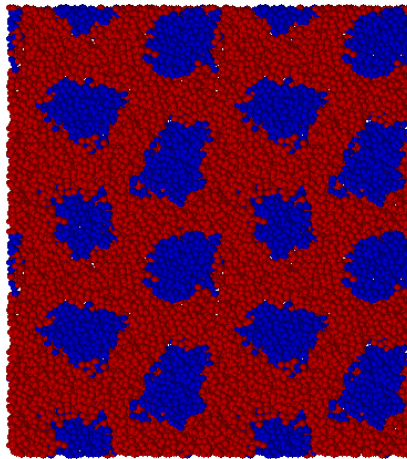


FIG. 6: Thin film of asymmetric block copolymer chains forming a hexagonal cylinder morphology.

We continue our analysis by investigating the behavior of this cylindrical forming block

copolymer on striped nanopatterned surfaces where each stripe is preferential to one block and repulsive to the other. The two stripes are symmetric with  $W = \frac{L_S^A}{L_S} = 0.5$  where  $W$  is the stripe asymmetry,  $L_S^A$  the thickness of a stripe preferential to the  $A$  part of the block copolymer chain and  $L_S$  the thickness of the pattern period. The pattern periods of the surface were chosen equal to the cylinder to cylinder spacing. The thickness of the film was varied and the equilibrium morphologies were obtained. Recently, Edwards et al. [39] have investigated these systems experimentally and have characterized with scanning electron microscopy the top part of these polymer films. However, the rest of the film cannot be characterized with these experimental techniques. With our simulations we attempt to verify and complement this analysis.

In Figure 7 the morphologies for different film heights are given. As we can see for a thickness commensurate to  $L_{cc} \cdot \sin(\frac{\pi}{3})/2$ , semicylinders are formed on the stripe patterns (Figure 7a,b). Increasing the film thickness, making it commensurate to  $L_{cc} \cdot \sin(\frac{\pi}{3})$ , the block copolymer thin film assembles to form a layer of defect free semicylinders at the patterned surface as previously and a second layer of semicylinders at the top surface both with the same repeat period equal to the cylinder to cylinder spacing and the chemical surface pattern (Figure 7c,d).

We continue our study for a system of film thickness  $27.2\sigma$  and we observe again the formation of semicylinders near the patterned surface and the appearance of defects further away. We additionally find the formation of cylinders perpendicular to the surface near the upper wall (Figure 8) in agreement with previous literature findings [40].

We saw the effect of film thickness on the self assembly of a cylindrical block copolymer on a patterned surface. Until now the stripe patterned surface was kept symmetric ( $W = 0.5$ ). By choosing a film of thickness  $L_{cc} \cdot \sin(\frac{\pi}{3})$ , we perform two calculations of asymmetrical stripes one of  $W = 0.45$  and a second of  $W = 0.55$ . For the system of  $W = 0.55$ , defects were found that consist mostly of unregistered cylindrical domains (Figure 9a). More interesting are the results for  $W = 0.45$ . As we can see from Figures 9b,c,d, some defects are apparent on the free surface of the film. However, if we look at a slab of the film slightly lower (height  $11.5\sigma$ ) than the free surface, we observe cylinders perpendicular to the surface. On the patterned surface a layer of semicylinders parallel to the stripes is found. These parallel semicylinders and the perpendicular cylinders are connected. We can see that while experiments such as scanning electron microscopy can provide us with a clear view of the

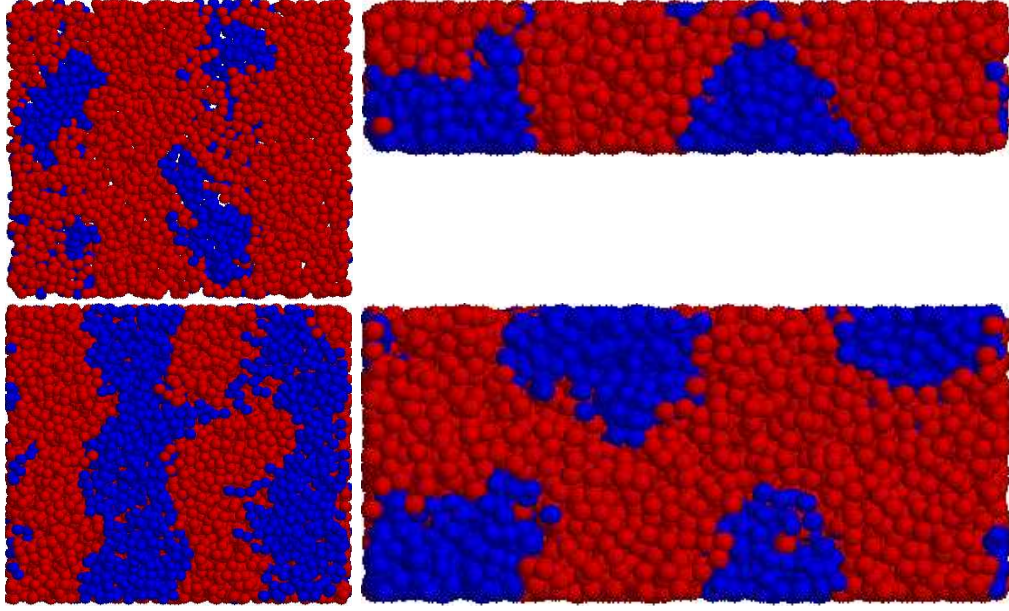


FIG. 7: Morphology change of asymmetric block copolymer chains on patterned surfaces, with pattern periods equal to the cylinder to cylinder spacing and varying the height of the film. The top and sideview of the systems is plotted. Thickness: a,b)  $7\sigma$  or  $L_{cc} \cdot \sin(\frac{\pi}{3})/2$ , c,d)  $13.6\sigma$  or  $L_{cc} \cdot \sin(\frac{\pi}{3})$

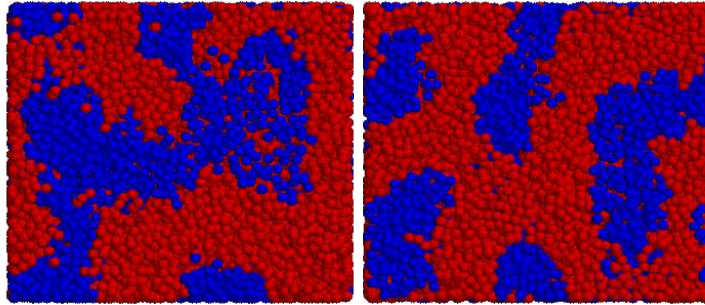


FIG. 8: Morphology change of asymmetric block copolymer chains on patterned surfaces, with pattern periods equal to the cylinder to cylinder spacing for higher film thickness. a) Sideview of a systems of thickness  $27.2\sigma$  or  $2 \cdot L_{cc} \cdot \sin(\frac{\pi}{3})$  b) Topview of a systems of thickness  $27.2\sigma$  or  $2 \cdot L_{cc} \cdot \sin(\frac{\pi}{3})$

free surface of the film, simulations are necessary to characterize the self assembly through the material.

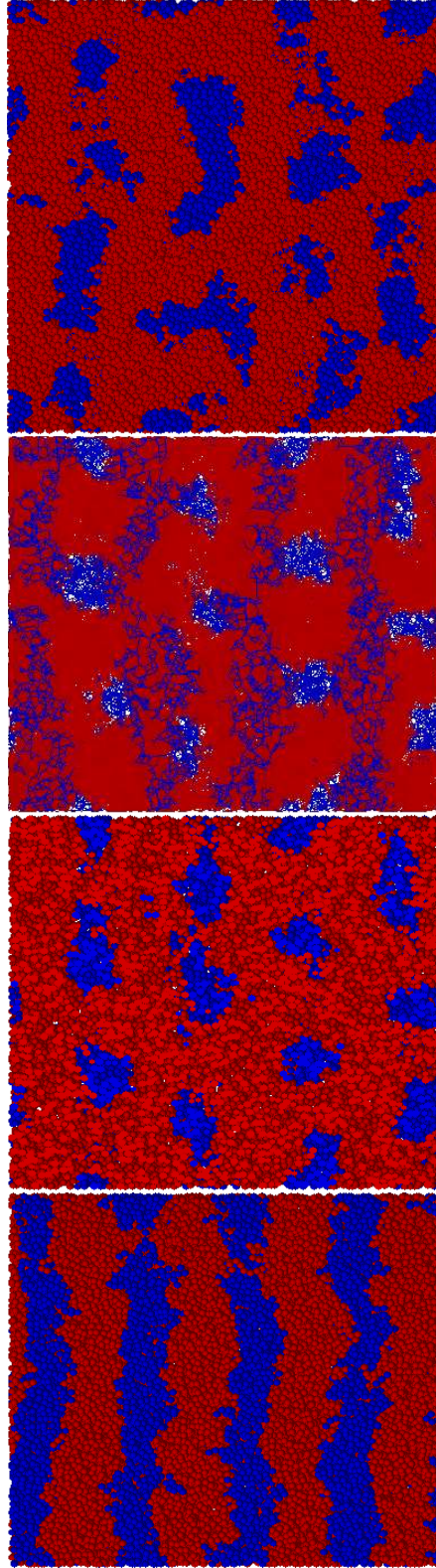


FIG. 9: Captions of self assembled cylindrical domains in a  $13.6\sigma$  thickness block copolymer film. a) Top view of a system of stripe asymmetry  $W = 0.55$ . b) Top view of a system of stripe asymmetry  $W = 0.45$ . c) Slab of the film at height  $11.5\sigma$  d) Bottom view of a system of stripe asymmetry  $W = 0.45$ .

## V. CONCLUSIONS

We have described a technique, that allows us to map a coarse grained model exactly to theory and connect it to a realistic experimental system. For this procedure three variables are necessary to be estimated: the Flory-Huggins parameter,  $\chi N$ , which is a measure of the incompatibility of different type of segments, the end-to-end distance of the blockcopolymer chain  $R_e$  for the length scaling, and the invariant degree of polymerization  $\bar{N}$  related to the strength of the fluctuations. For blockcopolymer chains under confinement one extra parameter has to be determined, which describes the strength of the polymer segment-surface interaction controlled by  $\Lambda N$ .

It has to be mentioned that, most commonly for experiments and coarse grained models, the random phase approximation (RPA) [32] is used in order to obtain the value of  $\chi$  for a system. It has been shown, though, that an alteration of the end to end distance is apparent with variance of interaction strength [41], suggesting that the RPA is not accurate. In addition, our verification that  $\chi$  can depend non-linearly on temperature suggests that RPA usage under the assumption that a linear temperature dependence exists can lead to incorrect results. The same is true for other techniques, such as the one-fluid approximation [23], that are used to obtain a value of  $\chi$  in the disordered regime and then extrapolate the value of  $\chi N$  in the ordered regime. This method will not be accurate because of the non-linearity of  $\chi$  with temperature. The Flory Huggins lattice model is indeed an oversimplification. However, mapping the results on it is necessary for a connection of experiments and simulations. The procedures that we presented outputs the values for the Lennard Jones parameters in order for our bead spring model to represent a specific value of  $\chi N$  in the Flory Huggins theory.

We have presented results of microphase separation of block copolymer chains on surfaces and we found well agreement with experiments. Lamellae structures, formed on stripe patterned surfaces, were able to accommodate mismatch between the block copolymer lamellae period and the surface spacing. A compression or expansion of 10% gave perfect lamellae without defects. For higher compressions or extensions, defects became apparent.

A different region of the phase diagram of the bulk block copolymer was also investigated where by appropriately selecting the chain asymmetry and value of Lennard Jones parameters we captured the cylinder phase. After obtaining the hexagonal cylinder morphology, we calculated the equilibrium cylinder to cylinder spacing. The self assembly of this system

on striped patterned surfaces of varying stripe symmetries and for different film thicknesses was studied.

The coarse grained model described in this paper successfully captures experimentally observed behaviors and it can be used to represent specific realistic systems even if no atomistic details are accounted for. This method can be used to obtain the values for the required parameters and then one has the liberty to choose either Monte Carlo or molecular dynamics simulations to study a problem. In our work we chose a Monte Carlo algorithm to investigate the microphase separation. By implementing the double bridging move we can efficiently sample the systems under study. On the other hand, molecular dynamics can be utilized, after the bead spring model is mapped, to investigate the dynamics of the self-assembly.

## VI. ACKNOWLEDGMENTS

This work is supported by NSF. Partial support from the Semiconductor Research Corporation (SRC) is also gratefully acknowledged.

- 
- [1] M. Rubinstein and R. Colby, *Polymer Physics* (Oxford University Press, 2003), 1st ed.
  - [2] W.A.Lopes and H. Jaeger, *Nature* **414**, 735 (2001).
  - [3] A. Edrington, A. Urbas, P. DeRege, C. Chen, T. Swager, N. Hadjichristidis, M. Xenidou, L. Fetters, J. Joannopoulos, Y. Fink, et al., *Adv. Mat.* **13**, 421 (2001).
  - [4] C. Park, J. Cheng, M. Fasolka, A. Mayes, C. Ross, E. Thomas, and C. DeRosa, *Appl. Phys. Lett.* **79**, 848 (2001).
  - [5] J. Cheng, C. Ross, V. Chan, E. Thomas, R. Lammertink, and G. Vancso, *Adv. Mat.* **13**, 1174 (2001).
  - [6] G. Fredrickson, *The Equilibrium Theory of Inhomogeneous Polymers* (Oxford Science Publications, 2006), 1st ed.
  - [7] M. Muller and G. Smith, *Jour. Pol. Sci. Part B-Pol. Phys.* **43**, 934 (2005).
  - [8] K. Daoulas, M. Muller, M. Stoykovich, S. Park, G. Papakonstantopoulos, J. de Pablo, Solak, and P. Nealey, *Phys. Rev. Lett.* **96**, 036104 (2006).

- [9] K. Daoulas and M. Muller, J. Chem. Phys. **125**, 184904 (2006).
- [10] D. Heine, D. Wu, J. Curro, and G. Grest, J. Chem. Phys. **118**, 914 (2003).
- [11] M. Kikuchi and K. Binder, J. Chem. Phys. **101**, 3367 (1994).
- [12] R. Larson, Macromolecules **27**, 4198 (1994).
- [13] Q. Wang, P. Nealey, and J. de Pablo, Macromolecules **35**, 9563 (2002).
- [14] Q. Wang, S. Nath, M. Graham, P. Nealey, and J. de Pablo, J. Chem. Phys. **112**, 9996 (2000).
- [15] P. Chen, X. He, and H. Liang, J. Chem. Phys. **124**, 104906 (2006).
- [16] F. Martinez-Veracoechea and F. Escobedo, Macromolecules **38**, 8522 (2005).
- [17] T. Geisinger, M. Muller, and K. Binder, J. Chem. Phys. **111**, 5241 (1999).
- [18] M. Muller, Macromol. Theory Simul. **8**, 343 (1999).
- [19] E. Reister, M. Muller, and K. Binder, Phys. Rev. E **64**, 041804 (2001).
- [20] A. Schultz, C. Hall, and J. Genzer, J. Chem. Phys. **117**, 10329 (2002).
- [21] A. Alsunaidi and B. Abu-Sharkh, J. Chem. Phys. **119**, 9894 (2003).
- [22] R. Groot and T. Madden, J. Chem. Phys. **108**, 8713 (1998).
- [23] G. Grest, M. Lacasse, K. Kremer, and A. Gupta, J. Chem. Phys. **105**, 10583 (1996).
- [24] M. Murat, G. Grest, and K. Kremer, Macromolecules **32**, 595 (1999).
- [25] B. Banaszak and J. de Pablo, J. Chem. Phys. **119**, 2456 (2003).
- [26] G. Papakonstantopoulos, K. Yoshimoto, M. Doxastakis, P. Nealey, and J. de Pablo, Phys. Rev. E **72**, 031801 (2005).
- [27] N. Karayiannis, V. Mavrantzas, and D. Theodorou, Phys. Rev. Lett. **88**, 105503 (2002).
- [28] K. Daoulas, M. Muller, M. Stoykovich, S. Park, G. Papakonstantopoulos, J. de Pablo, Solak, and P. Nealey, Journal of Polymer Science Part B: Polymer Physics **44**, 2589 (2006).
- [29] M. Stoykovich, M. Muller, S. Kim, H. Solak, E. Edwards, J. de Pablo, and P. Nealey, Science **308**, 1442 (2005).
- [30] S. Kim, H. Solak, M. Stoykovich, N. Ferrier, J. de Pablo, and P. Nealey, Nature **424**, 411 (2003).
- [31] A. Costa, M. Geoghegan, P. Vlcek, and R. Composto, Macromolecules **36**, 9897 (2003).
- [32] P.-G. de Gennes, *Scaling Concepts in Polymer Physics* (Cornell University Press, 1979), 1st ed.
- [33] Z. Sun, L. An, H. Li, Z. Jiang, and Z. Wu, Macromol. Theory and Simulations **10**, 692 (2001).
- [34] M. Kamal, N. DeMarquette, R. LaiFook, and T. Price, Polymer Engin. and Science **37**, 813

- (1997).
- [35] G. Fredrickson, “*Thermodynamics of Polymer Blends*”, *Physical Properties of Polymers Handbook, Chapter 19* (AIP Press, New York, 1996).
  - [36] S. Stryuk and B. Wolf, cond-mat/0306195 (2003).
  - [37] H. Lee, W. Kim, and C. Burns, *J. Appl. Polym. Sci.* **64**, 1301 (1997).
  - [38] M. Sferrazza, C. Xiao, R. Jones, D. B. J. Webster, and J. Penfold, *Phys. Rev. Lett.* **78**, 3693 (1997).
  - [39] E. Edwards, M. Stoykovich, H. Solak, and P. Nealey, *Macromolecules* **39**, 3598 (2006).
  - [40] Q. Wang, P. Nealey, and J. de Pablo, *Macromolecules* **36**, 1731 (2003).
  - [41] A. Sariban and K. Binder, *Macromolecules* **21**, 711 (1988).